

Synthesizing Tensor Transformations for Visual Self-attention

Xian Wei*, Xihao Wang¹, Hai Lan^{2,3}, JiaMing Lei³,
Yanhui Huang⁴, Hui Yu⁵, Jian Yang⁶

xian.wei@tum.de*, xihao wang2016@gmail.com¹, lanhai09@fjirsm.ac.cn², scutwhite@gmail.com³,
huangyanhuind@gmail.com⁴, yuhui@fjirsm.ac.cn⁵, jyangtum@qq.com⁶

Abstract

Self-attention shows outstanding competence in capturing long-range relationships while enhancing performance on vision tasks, such as image classification and image captioning. However, the self-attention module highly relies on the dot product multiplication and dimension alignment among query-key-value features, which cause two problems: (1) The dot product multiplication results in exhaustive and redundant computation. (2) Due to the visual feature map often appearing as a multi-dimensional tensor, reshaping the scale of the tensor feature to adapt to the dimension alignment might destroy the internal structure of the tensor feature map. To address these problems, this paper proposes a self-attention plug-in module with its variants, namely, Synthesizing Tensor Transformations (STT), for directly processing image tensor features. Without computing the dot-product multiplication among query-key-value, the basic STT is composed of the tensor transformation to learn the synthetic attention weight from visual information. The effectiveness of STT series is validated on the image classification and image caption. Experiments show that the proposed STT achieves competitive performance while keeping robustness compared to self-attention based above vision tasks.

1 Introduction

In recent years, the attention mechanism is generating considerable interest in the domain of deep learning. The main breakthroughs of attention modules were first appeared in Natural Language Processing (NLP) [33, 45, 41, 24, 43, 8, 32], and then also in com-

puter vision domain [47, 20, 14]. These achievements have demonstrated that the attention module provided a different approach than Convolutional Neural Network (CNN) models to handle the task and demonstrated a promising performance.

Generally, the attention module tends to exert a learnable weight on features to distinguish importance from various perspectives. According to the computing techniques and tasks, the attention modules can be categorized into two types. Hard attention module is non-differentiable and requires computation tricks [28, 1], while soft attention module is differentiable thus having wider applications for visual tasks [39, 19, 42]. As a particular form of attention, self-attention is applied as the core mechanism of the neural network named transformer, which is widely employed in the field of computer vision. The essential advantage of self-attention is that it focuses on the relative importance of own content rather than weighting across multiple contents as a general attention mechanism. As one of the critical roles in the self-attention mechanism, dot product multiplication among the feature of query, key, and value plays a significant role in learning self-alignment[35]. Precisely, employing the dot product between a single token and all other tokens in the sequence could formulate the relative importance score. Through pairwise dot product, the self-attention mechanism establishes a content-based retrieval process.

However, do we really need to use dot product in the self-attention mechanism? Is it the best choice to learn the self-alignment between the features of query and key? We can not deny that attention-based architecture is one of the most efficient models in machine learning, but it also has space to improve[12]. Investigating the alternative plug-in module for current architecture could help us to have a deeper un-

*Corresponding Author

derstanding of the attention mechanism. Undoubtedly, dot product multiplication has several benefits. But it also induces exhaustive and redundant computation during exerting on the features. Especially on large-scale processing data, the extra parameters and memory caused by dot product operations enormously increase the burden of the training process. Moreover, in the computer vision task, self-attention for images tends to compute the similarity scores among visual features[47, 42, 27] rather than mapping for retrieval. In order to overcome the shortages of dot production, it is necessary to search for another approach to improve the performance of the self-attention mechanism. As the result, recent findings regarding the NLP attention module have led to an alternative approach, named Synthesizer Attention[35].

In our work, we provide a viable alternative to overcome the shortage brought from the dot-production in the standard self-attention module, in order to pursue a better performance of visual self-attention. Inspired by the NLP-like synthesizer, we propose a plug-in synthesizer to replace traditional visual self-attention modules, namely, the Visual Dense Synthesizing (VDS) module. Compared with the NLP-like synthesizer, which contains one-dimensional natural language vectors, our module applies the multi-dimensional tensor to adapt the presentation of visual features. The module is basically composed of a tensor transformation for self-alignment between query matrix and key matrix, without computing the dot-product multiplication among the feature of query-key-value. Removing dot product operations, the VDS gains some straightforward advantages.

1. Replacing dot production based computation with a learnable linear synthesizer reduces dependency on the input, thus enhancing the robustness of the model against external perturbations.
2. The proposed linear synthesizer can be easily adapted to input data structure, without reshaping the raw input. Thus, it is easier to preserve the underlying structure of feature maps.
3. Since the alignment transformations in the syn-

thesizer are computed upon various dimensions of feature maps, the attention is produced simultaneously in both channel and spacial domain.

To further simplify the linear transformations in synthesizing, derived from the regular VDS module, the paper further proposes a series of plug-and-play modules, namely, Synthesizing Tensor Transformations (STT). The STT series are finally applied for the image classification task and image caption task. According to the result of our typical classification experiment, the STT series demonstrates that it not only is a viable alternative of the traditional self-attention module but also has better robustness.

2 Related Work

In this section, we will introduce the various applications of the self-attention mechanism. Then, the dot product in self-attention would be described as the preliminaries for our STT series.

2.1 Self-Attention Mechanism

The self-attention attracts considerable interest due to its versatile application. For CNN-based models, self-attention mechanism has been used in many modules, such as extra re-weighting modules for channels [18, 19, 39], jointly spatial and channel attention module [4, 42, 15], or remold convolution operation with self-attention [2, 29, 9, 46].

Another line of works arrange self-attention to be a component in a pipeline for downstream tasks, such as augmentation of feature maps for classification [2], object detection [47, 17, 3], and segmentation [40]. However, it is difficult to directly apply the self-attention mechanism to pixel-wise data. [30] restricted self-attention convolution within local neighborhoods for query pixels, and [40, 16] restricted computation along individual axes. [5] reduced image resolution and color space before transformer, and [13] directly applied transformer on image sequence patches.

To reduce computational costs, some of the work adjust the structure of attention. [21] divided and permuted the feature map thus smaller attention map

would be conquered and permuted back. [22] focused on the criss-cross around the key points on the feature of query, key and value. [7] adopted double attention to re-allocate features for channels and the total workload shrinks after feature gathering. Differently, another way is to reduce the length at certain dimension [41], or divide computation by locality sensitive hashing [24].

2.2 Dot-product in Self-attention

The regular self-attention operator based dot-product attention serves as a basic building block of vision tasks [2, 29, 9, 46]. Let $\mathcal{X} \in \mathbb{R}^{H \times W \times C}$ be a tensor input with the height H , the width W , the number of channels C .

To feed the self-attention block, the 3D tensor $\mathcal{X} \in \mathbb{R}^{H \times W \times C}$ is first flattened to a 2D matrix $X \in \mathbb{R}^{HW \times C}$. Then X is projected to corresponding representations Q , K and V , with $Q = \phi_Q(X)$, $K = \phi_K(X)$ and $V = \phi_V(X)$, respectively. ϕ_Q, ϕ_K, ϕ_V are trainable transformations such as linear mappings or convolutions, and have matching output dimensionality. For example, if we read ϕ_Q, ϕ_K, ϕ_V are linear transformations $W_Q \in \mathbb{R}^{C \times d}$, $W_K \in \mathbb{R}^{C \times d}$ and $W_V \in \mathbb{R}^{C \times d}$, respectively, the representations are $Q = XW_Q$, $K = XW_K$, $V = XW_V$, and m means the desired output dimension. Finally, the output value is weighted average over input values,

$$S = \text{Softmax} \left(\frac{QK^\top}{\sqrt{d}} \right) \quad (1)$$

$$Y = \text{Attention}(Q, K, V) = SV. \quad (2)$$

Where S denotes the attention coefficients that S_{ij} measures the similarity between the i^{th} row of Q and the j^{th} row of K . The detail of the dot-production is presented in the Figure 1a.

3 Synthesizing Tensor Transformation

In order to introduce our Synthesizing Tensor Transformation, we first give a fundamental model of tensor synthesizer. And then, the specific tensor synthesizers would be provided as (a) Tensor Dense Synthesizer,

(b) Tensor Random Synthesizer, and (c) Tensor Factorized Synthesizer.

3.1 Preliminaries

Basic Tensor Synthesizer As shown in Section 2.2, given a tensor input $\mathcal{X} \in \mathbb{R}^{H \times W \times C}$ and its 2D reshaped matrix $X \in \mathbb{R}^{HW \times C}$, the dot-product self-attention could be interpreted as producing a dimension alignment from $\mathbb{R}^{HW \times C}$ to $\mathbb{R}^{HW \times HW}$. In the case of regular visual transformation architecture, it will reshape the input feature X as a defined dimensional vector [13]. However, it may result in the loss of spatial information and a prohibitively expensive computation when the dimension is high. Thus, in order to directly process the tensor input $\mathcal{X} \in \mathbb{R}^{H \times W \times C}$, we propose to synthesize tensor transformation for replacing the dot-product self-attention in this section.

Formally, let $\mathcal{O} \in \mathbb{R}^{H \times W \times d}$ be the projected features of $\mathcal{X} \in \mathbb{R}^{H \times W \times C}$ via the mapping $\mathcal{F} = (\cdot)$, where C and d are the number of channels.

$$Z = \mathcal{F}(\mathcal{O}), \quad (3)$$

Intuitively, the $\mathcal{F} = (\cdot)$ could be a 3^{rd} tensor product. In detail, the mapping $\mathcal{F}(\cdot)$ could be composed by three layered feed-forward network, as followed:

$$\mathcal{F}(\mathcal{O}) = \mathcal{O} \times_1 \mathbf{A}_{(H)} \times_2 \mathbf{A}_{(W)} \times_3 \mathbf{A}_{(C)} \quad (4)$$

with $\mathbf{A}_{(H)}$, $\mathbf{A}_{(W)}$, and $\mathbf{A}_{(C)}$ are three tensors. For a detailed introduction of tensor products, we refer the interested reader to [10, 36, 34].

Definition 1. Given the tensor $\mathcal{X} \in \mathbb{R}^{I_1 \times I_2 \times \dots \times I_N}$ and the matrix $\mathbf{A} \in \mathbb{R}^{J_n \times I_n}$, the n -mode product is denoted by

$$\mathcal{X} \times_n \mathbf{A} \quad (5)$$

and results in a $I_1 \times I_2 \times \dots \times I_{n-1} \times J_n \times I_{n+1} \times \dots \times I_N$ tensor. The entries of this tensor are defined as

$$(\mathcal{X} \times_n \mathbf{A})_{i_1 i_2 \dots i_{n-1} j_n i_{n+1} \dots i_N} = \sum_{i_n=1}^{I_n} x_{i_1 i_2 \dots i_n} \cdot a_{j_n i_n} \quad (6)$$

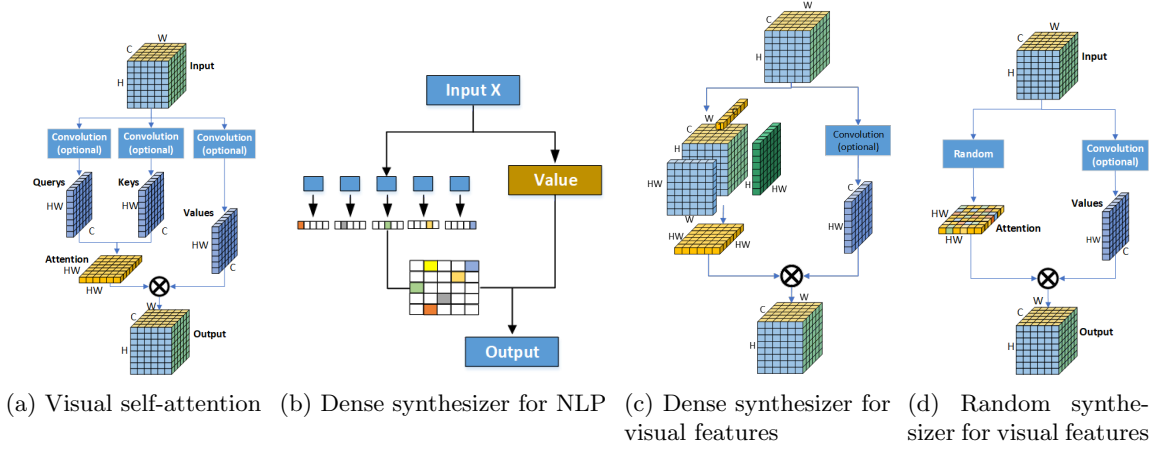
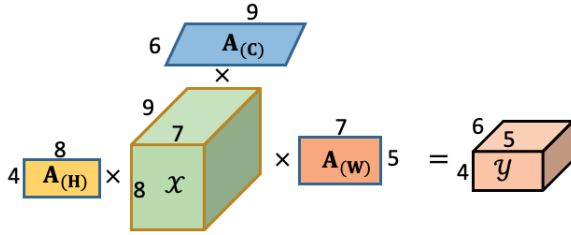


Figure 1: Classical visual self-attention vs. Synthesizers.



for all $j_n = 1, \dots, J_n$.

For the convenience of understanding the tensor product, Figure 2 illustrates an example of n -mode production. Besides, in order to obtain an appropriate size of the matrix, a method named *n-mode matrix unfolding* is required. Depending on this method, we are able to build the layered feed-forward network as Eq. (4). The multiplication of a k -way tensor \mathcal{X} along all its modes with matrices A_1, \dots, A_k [34]

$$\mathcal{Y} = \mathcal{X} \times_1 A_1 \times_2 A_2 \times_3 \dots \times_k A_k \quad (7)$$

can be rewritten as the following linear system:

$$\text{vec}(\mathcal{Y}) = (A_k \otimes \dots \otimes A_2 \otimes A_1) \text{vec}(\mathcal{X}) \quad (8)$$

where $\text{vec}(\cdot)$ means the vector space isomorphism $\text{vec}: \mathbb{R}^{a \times b} \rightarrow \mathbb{R}^{ab}$, which denotes the operator that stacks the columns of a matrix below one another [34]. Therein, \otimes denotes the Kronecker product operator, with which the Kronecker product of \mathbf{A} and \mathbf{B} is defined by

$$\mathbf{A} \otimes \mathbf{B} = \begin{bmatrix} A_{11}\mathbf{B} & \dots & A_{1k_1}\mathbf{B} \\ \vdots & \ddots & \vdots \\ A_{a_1}\mathbf{B} & \dots & A_{ak_1}\mathbf{B} \end{bmatrix} \quad (9)$$

with A_{ij} being an entry in \mathbf{A} . Therefore, the mapping $\mathcal{F} = (\cdot)$ could be presented as the tensor multiplication as the Eq. 4. To offer a better understanding for this definition, Figure 3 shows the process of the tensor multiplication with Kronecker product operator.

3.2 Synthesizer Tensor Model

Tensor Dense Synthesizer To achieve mentioned dimension alignment on raw tensor \mathcal{O} without the dot-product self-attention mechanism, we define a tensor transformation to compute attention coefficients by replacing the dot-product self-attention, as follows,

$$Z = \mathcal{O} \times_1 \mathbf{A}_{(H)}^{(l)} \times_2 \mathbf{A}_{(W)}^{(l)} \times_3 \mathbf{A}_{(C)}^{(l)}, \quad (10)$$

$$S = \text{Softmax}(Z) \quad (11)$$

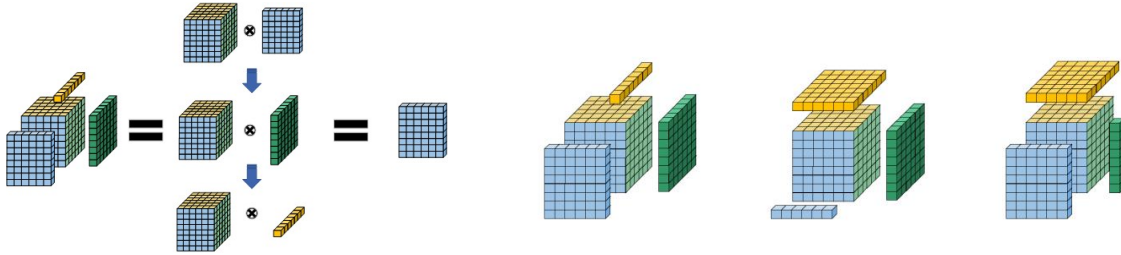


Figure 3: Illustrations for tensor multiplication and decomposition.

with $\mathbf{A}_{(H)}^{(l)} \in \mathbb{R}^{HW \times H}$, $\mathbf{A}_{(W)}^{(l)} \in \mathbb{R}^{HW \times W}$, $\mathbf{A}_{(C)}^{(l)} \in \mathbb{R}^{1 \times d}$, $Z \in \mathbb{R}^{HW \times HW \times 1}$ and $S \in \mathbb{R}^{HW \times HW \times 1}$, and l denotes the layer number. The combination of Eq. (10) and Eq. (11) is referred to the VDS module in Section 1. Then, the output is computed by

$$Y = \text{Synthesizer}(Q, V) = SV. \quad (12)$$

This approach eliminates the dot product altogether by replacing QK^\top in standard self-attention with the synthesizing function defined in Eq. (11).

Tensor Random Synthesizer In the model of Tensor Dense Synthesizer, the features of input are projected from $\mathcal{X} \in \mathbb{R}^{H \times W \times C}$ to HW dimensions via the 3^{rd} tensor production. Intuitively, the synthesizer implements the conditioning on each feature independently. In contrast, the Tensor Random Synthesizer utilizes the random value as initialized attention weights. Then, the attention weights could follow the training process to update, or keep fixed.

Since the synthesizer can be regarded as a self-alignment of dimensions, we can make an attempt to set Z as a random matrix. And the Random Synthesizer is defined as:

$$Y = \text{Synthesizer}(Q, V) = \text{Softmax}(R)V, \quad (13)$$

with $R \in \mathbb{R}^{HW \times HW}$ being a randomly initialized matrix. The attempt of utilizing the random initial matrix identifies the idea that it is unnecessary to rely on any information from the individual input feature. Therefore, the Random Tensor Synthesizer is tending to learn the task-specific alignment through the

training process. According to the token-token self-attention, it is able to handle the cases that exceed length $H \times W$. In our work, the factorized approach will address this case, and we will introduce it in the Section 3.3.

Definition 2. If a tensor $\mathcal{Y} = \mathcal{X} \times_1 \mathbf{A}_{(1)} \times_2 \mathbf{A}_{(2)} \times_3 \mathbf{A}_{(3)}$ with $\mathcal{Y} \in \mathbb{R}^{I_1 \times I_2 \times I_3}$, it could be assigned the dimension to three transformations. Therein, $\mathcal{Y}_1, \mathcal{Y}_2, \mathcal{Y}_3$ are computed as follows.

$$\mathcal{Y}_1 = \mathcal{X} \times_1 \mathbf{A}_{(1)} \times_2 \mathbf{A}_{(2)} \times_3 \mathbf{A}_{(3)}$$

with $\mathbf{A}_{(1)} \in \mathbb{R}^{1 \times I_1}$, $\mathbf{A}_{(2)} \in \mathbb{R}^{I_1 \times I_2 \times I_2}$, $\mathbf{A}_{(3)} \in \mathbb{R}^{I_1 \times I_2 \times I_3}$.

$$\mathcal{Y}_2 = \mathcal{X} \times_1 \mathbf{A}_{(1)} \times_2 \mathbf{A}_{(2)} \times_3 \mathbf{A}_{(3)}$$

with $\mathbf{A}_{(1)} \in \mathbb{R}^{I_1 \times I_2 \times I_1}$, $\mathbf{A}_{(2)} \in \mathbb{R}^{1 \times I_2}$, $\mathbf{A}_{(3)} \in \mathbb{R}^{I_1 \times I_2 \times I_3}$,

$$\mathcal{Y}_3 = \mathcal{X} \times_1 \mathbf{A}_{(1)} \times_2 \mathbf{A}_{(2)} \times_3 \mathbf{A}_{(3)}$$

with $\mathbf{A}_{(1)} \in \mathbb{R}^{I_1 \times I_2 \times I_1}$, $\mathbf{A}_{(2)} \in \mathbb{R}^{I_1 \times I_2 \times I_2}$, $\mathbf{A}_{(3)} \in \mathbb{R}^{1 \times I_3}$.

It is difficult to determine the dimensions of $\mathbf{A}_{(H)}^{(l)}$, $\mathbf{A}_{(W)}^{(l)}$, $\mathbf{A}_{(C)}^{(l)}$, i.e., how to assign the dimensions $HW, H, W, 1$ to three transformations. We note that all of the proposed synthetic attention variants can be mixed in an additive fashion. Depending on the definition, Eq. (11) can be expressed as:

$$\begin{aligned} S &= \text{Softmax}(Z_H)V = \text{Softmax}(Z_W)V \\ &= \text{Softmax}(Z_C)V. \end{aligned} \quad (14)$$

For example, Z_H could be computed as follows:

$$Z_H = \mathcal{O} \times_1 \mathbf{A}_{(H)}^{(l)} \times_2 \mathbf{A}_{(W)}^{(l)} \times_3 \mathbf{A}_{(C)}^{(l)}$$

with $\mathbf{A}_{(H)}^{(l)} \in \mathbb{R}^{1 \times H}$, $\mathbf{A}_{(W)}^{(l)} \in \mathbb{R}^{HW \times W}$, $\mathbf{A}_{(C)}^{(l)} \in \mathbb{R}^{HW \times d}$. In Figure 3, we offer the visualization plot to describe this definition.

3.3 Multiple-level Factorized Tensor Synthesizer

We replace the dot-production in the standard self-attention module with our synthesizer module in the Tensor Dense Synthesizer. However, the synthesizer is too burdensome to learn when the size of parameters is too large. As shown from Eq. (11), the basic 3rd tensor synthesizer contains several parameters $\mathbf{A}_{(H)}^{(l)} \in \mathbb{R}^{HW \times H}$, $\mathbf{A}_{(W)}^{(l)} \in \mathbb{R}^{HW \times W}$, $\mathbf{A}_{(C)}^{(l)} \in \mathbb{R}^{d \times 1}$. Therefore, there are several factorized tensor synthesizer models introduced.

Tensor Dense Factorized Synthesizer In order to reduce the size of parameters, partially avoiding the overfitting while HW being huge, the parameter matrices could be decomposed w.r.t the Kronecker product[36]. The decomposition can be conducted on three dimensions of the feature map, as can be seen in Figure 3.

For example, $\mathbf{A}_{(H)}^{(l)}$ could be approximated by N small matrices as

$$\mathbf{A}_{(H)}^{(l)} = \mathbf{A}_{(H)_1}^{(l)} \otimes \mathbf{A}_{(H)_2}^{(l)} \otimes \cdots \otimes \mathbf{A}_{(H)_N}^{(l)}, \quad (15)$$

where $\mathbf{A}_{(H)_i}^{(l)} \in \mathbb{R}^{\alpha_i \times \beta_i}$ with α_i, β_i being dimensions, $HW = \alpha_1 \alpha_2 \cdots \alpha_N$, $H = \beta_1 \beta_2 \cdots \beta_N$. By using the Kronecker product operator, $\mathbf{A}_{(H)}^{(l)}$, $\mathbf{A}_{(W)}^{(l)}$, $\mathbf{A}_{(C)}^{(l)}$ can be easily factorized to several very small matrices. The Tensor Dense Factorized Synthesizer is defined as:

$$Y = \text{Synthesizer}(Q, V) = \text{Softmax}(C)V. \quad (16)$$

Where $C = \mathcal{F}_H(\mathbf{A}_{(H)}^{(l)}) \times \mathcal{F}_W(\mathbf{A}_{(W)}^{(l)}) \times \mathcal{F}_C(\mathbf{A}_{(C)}^{(l)})$, $\mathcal{F}(\cdot)$ means the decomposition of the tensor and $C \in \mathbb{R}^{HW \times HW}$.

Tensor Random Factorized Synthesizer Similarly, the factorized synthesizer could also be applied

into Tensor Random Synthesizer. The idea is decomposing the matrix R into several low rank matrices $R_i \in \mathbb{R}^{\alpha_i \times \beta_i}$.

$$Y = \text{Synthesizer}(Q, V) = \text{Softmax}(\mathcal{R})V, \quad (17)$$

Where $\mathcal{R} = R_1 \otimes R_2 \otimes \cdots \otimes R_N$, and $\mathcal{R} \in \mathbb{R}^{HW \times HW}$. About the low rank matrices R_i , $\alpha_1 \alpha_2 \cdots \alpha_N = HW$, $\beta_1 \beta_2 \cdots \beta_N = HW$, and $\alpha_i, \beta_i \ll HW$. With the reduced size of parameters, it is able to avoid the overfitting problem.

Mixture Tensor Synthesizer After introduced the above three kinds of tensor synthesizer models, it raises a compounded model being the synthesizers mixed in additive fashion. For instance:

$$Y = \text{Softmax}(\theta_1 S_1(\mathcal{O}) + \cdots + \theta_N S_N(\mathcal{O}))V, \quad (18)$$

Where θ_i are the learnable weights, and $\sum_1^N \theta_i = 1$. S_i are the different synthesizer models. In the following experiment part, the Mixture Tensor Synthesizer composes Tensor Random Factorized Synthesizer and Tensor Dense Synthesizer together. The expression could be outlined as follow:

$$Y = \text{Softmax}(\theta_1 \mathcal{R} + \theta_2 Z)V, \quad (19)$$

Where Z is presented in Eq. (10). By employing more than one kind of synthesizer, it is possible to obtain a better performance than a composed individual synthesizer.

4 Experiments

In this section, we investigate the performance of our proposed STT module series on basic image classification. The experiments focus on the performance of the robustness of the model. For convenience, we abbreviate the proposed STT series and comparison methods. The detail of information are listed in Table 4.

| Model | None | CT | L | SD | SR | FSR | FSD | MS | STT | STTH | STTW |
|----------|-------|------|-------|-------|-------|-------|-------|-------|-------|-------|-------|
| Accuracy | 65.56 | 66.1 | 66.21 | 67.12 | 66.97 | 66.79 | 66.57 | 66.21 | 66.69 | 66.82 | 66.27 |

Table 1: The Accuracy of Each Model.

| Noise | 0.01 | 0.02 | 0.03 | 0.05 | 0.04 | 0.06 | 0.07 | 0.08 | 0.09 | 0.1 |
|-------|-------------|--------------|--------------|--------------|--------------|--------------|--------------|--------------|--------------|--------------|
| None | 45.96 | 34.35 | 27.8 | 22.83 | 20.01 | 17.86 | 16.23 | 15.07 | 14.45 | 13.76 |
| CT | 47.02 | 35.83 | 29.21 | 24.7 | 21.49 | 19.33 | 17.41 | 16.51 | 15.42 | 14.8 |
| L | 41.51 | 28.54 | 21.69 | 18.56 | 16.16 | 14.53 | 13.57 | 12.41 | 12.17 | 11.5 |
| SD | 48.71 | 37.79 | 31.54 | 27.3 | 23.7 | 22.23 | 20.18 | 18.92 | 17.45 | 17.03 |
| SR | 45.93 | 34.02 | 27.06 | 23.01 | 19.91 | 17.36 | 16.02 | 14.93 | 13.93 | 13.4 |
| FSR | 46.51 | 37.28 | 31.69 | 27.56 | 24.14 | 22.6 | 20.62 | 19.75 | 18.25 | 17.76 |
| FSD | 68.9 | 37.5 | 30.42 | 25.89 | 22.85 | 20.7 | 19.33 | 17.91 | 16.87 | 16.07 |
| STT | 47.29 | 36.81 | 31.98 | 28.11 | 25.49 | 23.75 | 22.39 | 21.44 | 20.09 | 19.54 |
| STTH | 44.66 | 30.92 | 23.26 | 19.58 | 17.08 | 15.12 | 14.04 | 13.35 | 12.61 | 12.26 |
| STTW | 42.2 | 30.21 | 23.65 | 19.92 | 17.53 | 16.41 | 15.18 | 14.65 | 14.33 | 13.64 |
| MS | 48.2 | 36.8 | 29.55 | 25.13 | 21.45 | 19.34 | 17.74 | 16.61 | 15.76 | 15.26 |

Table 2: Classification Result on Images with Relatively Small Gaussian Noise.

| ABBR | Combination |
|------|--|
| None | Convolution Baseline |
| CT | CNN + Transformer [37] |
| L | CNN + Linformer [41] |
| CNN | Double CNN |
| SD | CNN + Matrix Dense Synthesizer [35] |
| STT | CNN + Tensor Dense Synthesizer |
| SR | CNN + Tensor Random Synthesizer |
| STTH | CNN + Tensor Height Synthesizer |
| STTW | CNN + Tensor Width Synthesizer |
| FSD | CNN + Tensor Dense Factorized Synthesizer |
| FSR | CNN + Tensor Random Factorized Synthesizer |
| MS | CNN + Mixture Tensor Synthesizers |

Table 4: **Abbreviation of Model Zoo.** ABBR indicates abbreviations of our proposed STT series, with Double CNN being the convolution baseline followed by its repetition, Matrix Dense Synthesizer being the basic synthesizer proposed in [35], and Tensor Dense Synthesizer being our basic tensor synthesizer for vision tasks, Tensor Height Synthesizer being the tensor synthesizer with an attention map full-rank in height, and Mixture Tensor Synthesizer being the synthesizers mixed in additive fashion.

4.1 Image Classification

4.1.1 Implementation Details

STT series are validated on the benchmark image dataset CIFAR10[25] for classification. The CIFAR10 is composed by **10** classes, and it has **50000** images for training, **10000** for testing. To validate the functionality of the STT series as attention modules applied to a deep learning framework, we employed three different perturbations to test the model robustness of above all approaches. Applied perturbations are, namely, Gaussian noise, image rotations, and flipping.

1. Gaussian noise: random noise is added on every pixel of the input and we want to test whether the attention computed on the global scale outperforms the split ones.
2. Rotations and flips: once the rotations or flips are exerted, the order among channels would change correspondingly, while STT series treat the feature map on the whole.

| Rotation | 30 | 60 | 90 | 120 | 150 | 180 | 210 | 240 | 270 | 300 | 330 |
|----------|--------------|--------------|--------------|--------------|--------------|--------------|--------------|--------------|--------------|--------------|--------------|
| None | 37.58 | 26.51 | 23.07 | 21.12 | 19.4 | 19.39 | 18.68 | 18.89 | 18.27 | 17.74 | 17.4 |
| CT | 36.54 | 36.57 | 23.27 | 21.25 | 19.75 | 19.44 | 19.7 | 18.61 | 18.19 | 18.46 | 17.75 |
| L | 37.53 | 26.86 | 23.61 | 21.5 | 20.16 | 18.61 | 19.19 | 17.95 | 17.62 | 17.95 | 17.95 |
| SD | 37.9 | 38.64 | 23.24 | 21.79 | 19.26 | 19.45 | 19.36 | 18.51 | 17.55 | 17.6 | 17.98 |
| SR | 33.72 | 24.7 | 22.06 | 19.88 | 19 | 18.17 | 18.03 | 17.22 | 17.03 | 17.23 | 16.79 |
| FSR | 37.04 | 26.86 | 23.1 | 20.69 | 19.72 | 18.69 | 18.7 | 18.27 | 17.69 | 17.17 | 17.08 |
| FSD | 39.27 | 28.85 | 23.55 | 22.85 | 20.37 | 19.85 | 19.95 | 18.71 | 18.86 | 18.34 | 17.88 |
| MS | 37.91 | 26.93 | 22.96 | 21.74 | 19.61 | 18.89 | 18.76 | 18.01 | 18.06 | 17.62 | 17.65 |
| STT | 38.71 | 38.36 | 24.51 | 21.8 | 20.97 | 20.36 | 20.89 | 19.93 | 19.86 | 19.12 | 20 |
| STTH | 42.32 | 30.44 | 26.28 | 24.53 | 22.17 | 22.18 | 22.37 | 21.83 | 20.85 | 20.07 | 20.16 |
| STTW | 45.53 | 31.72 | 27.21 | 24 | 22.39 | 22.23 | 22.03 | 21.27 | 20.61 | 20.31 | 19.89 |

Table 3: Classification Result on Images with Rotations.

4.1.2 Ablation Study

To make fair comparisons with the traditional self-attention modules, we choose a two-layer CNN as the baseline. The evaluation metric is the classification accuracy. Besides, we select **Transformer**[37], **Linformer**[41], and **Matrix Dense Synthesizer**[35] to test their perturbation robustness in the same baseline structure.

About mentioned traditional self-attention modules, The **Transformer** and **Linformer** modules employ the dot-product to compute the similarity between token to token. And **Matrix Dense Synthesizer** also applies the synthesizer mechanism to replace the dot production, but it doesn’t leverage the basic tensor synthesizer in their module. Through the comparison, we could prove our STT series satisfy the requirement to become a valuable alternative to the dot-product-based self-attention model. Moreover, it has better robustness performance.

4.1.3 Quantitative Analysis on Robust Classification

According to our proposed STT series, one of the advantages mentioned in Section 1 is that they possess strong robustness against external perturbations. The reason is that they calculate attention maps without splitting the feature maps. Thus, the baseline model reduces the reliance on the input, and the underlying structure of the feature map has more possibility to preserved.

Our STT series has a more negligible effect from

external perturbation on the raw input than the dot-production-based self-attention modules. Hence, to evaluate the robustness validation for our proposed STT series, we conduct the image classification task to compare the STT series with traditional self-attention modules.

Image Classification Quantitative comparisons among various models are represented in the Table 1. We examine all the models mentioned in the Model Zoo, the results of accuracy are scarcely distinguishable from each model. According to the similar accuracy, our experiment demonstrates that our STT series have equal performance in the image classification task. Hence, the result proves that the dot-production mechanism is not the best choice for the self-attention module. The tensor synthesizer also shows the qualification to replace traditional dot-production as a valuable alternative. Although the results are similar under the no-noise situation, we focus on the ability to resist perturbation disturbance. Because the no-noise test only proves that the synthesizer module has the potential to replace the dot-production mechanism. The following robustness experiment would illustrate the unique advantage of the STT series.

Gaussian Noise As a common statistical noise caused by sensor during sampling or transmission, Gaussian noise is a widespread type of disturbance for digital images. Varied levels of Gaussian noises are

utilized to corrupt the images for robustness evaluation, with detailed settings and results being collected in Table 2.

As shown in Table 2, the accuracy of the classification decreases with the Gaussian noise increasing. Under the disturbance of Gaussian noise, the STT series doesn't represent the worse accuracy than the models with dot-production. In contrast, the STT series shows a more outstanding noise resistance. During the noise is still small, the **FSD** leads to the best result. With the noise becoming large, the **STT** keeps the highest accuracy than other modules. Among the STT series, the worse performance of **STTH** and **STTW** might result from the inferior representation because the information is only gathered from one side of the feature map compared to the transformer. Compared with the modules employing dot-product, synthesizing modules appear higher accuracy when Gaussian noise influences them.

Images with Rotations Rotations are common in image augmentation process. We apply rotations to the original images to test the robustness with the model pool. Detailed settings and results are recorded in Table 3.

In Table 3, it is obvious that the classification performance of the whole model zoo is impaired when rotation increases. However, the accuracy of the STT series represents a similar decreasing tendency. It proves that the STT series has the same performance as dot-production models when they are suffering the rotation noise. Despite the **STTH** and **STTW** modules, other approaches don't reveal the resistance of rotation noise. While transformer weakens the baseline CNN structure, **STTH** and **STTW** have a relatively better accuracy performance. Based on such result, we make an assumption that the full-rank attention map to give them a better robustness against the effect of rotation. This assumption could also explain that the **STT** has a relatively better result, because it also has a full-rank attention map.

| Module | horizon | vertical | ho+ve |
|--------|--------------|--------------|-------------|
| None | 64.74 | 25.18 | 25.08 |
| CT | 64.93 | 25.52 | 25.45 |
| L | 65.31 | 25.2 | 25.05 |
| SD | 65.7 | 25.08 | 25.21 |
| SR | 65.86 | 26.06 | 25.72 |
| FSR | 65.08 | 24.63 | 25.14 |
| FSD | 66.28 | 26.41 | 26.58 |
| MS | 65.6 | 25.75 | 25.99 |
| STT | 66.09 | 27.16 | 27.32 |
| STTH | 66.09 | 29.29 | 28.9 |
| STTW | 65.77 | 27.45 | 27.46 |

Table 5: Classification results on images with Flips, where ho+ve means that both horizontal and vertical flips are applied.

Robustness against Flipping The last perturbation is images flipping, which could be categorized into horizon flipping, vertical flipping, and flipping both in horizon and vertical. The results are recorded in Table 5.

From Table 5, we can see that accuracy decreases drastically once the vertical transformation is applied. Compared with the STT series and the traditional self-attention modules, their accuracy doesn't appear a distinguished difference. It demonstrates that the synthesizer modules are not more vulnerable under the flipping noise. Even though all the models have severe impair from vertical flipping noise, the STT series has slightly better accuracy.

4.2 Image Captioning

4.2.1 Implementation Detail

We report our results on Microsoft COCO-2014 [6] dataset with 82,783 images for training, 40,504 images for validation and 40,775 images for testing.

Encoder-Decoder Architecture To test the potency of STT series as a powerful alignment module and a substitution of transformer, the comparison of the series is all implemented with a common encoder-decoder architecture adopted in [44]. The only dif-

| Metric | BLEU-1 | BLEU-2 | BLEU-3 | BLEU-4 | METEOR | ROUGE | CIDEr |
|-------------|---------------|---------------|---------------|---------------|---------------|---------------|---------------|
| LSTM | 0.7191 | 0.5153 | 0.3468 | 0.2339 | 0.2725 | 0.5699 | 0.8128 |
| Transformer | 0.7077 | 0.5035 | 0.3392 | 0.2289 | 0.2692 | 0.5621 | 0.7970 |
| SD | 0.7921 | 0.6566 | 0.5386 | 0.4457 | 0.3686 | 0.7211 | 1.2099 |
| SR | 0.7888 | 0.6542 | 0.5359 | 0.4433 | 0.3688 | 0.7213 | 1.2040 |
| MS | 0.7925 | 0.6569 | 0.5383 | 0.4451 | 0.3691 | 0.7225 | 0.2104 |
| FSR | 0.7876 | 0.6505 | 0.5293 | 0.4345 | 0.3646 | 0.7159 | 1.1793 |

Table 6: Image captioning performance with Scaled-Dot-Product self-attention being replaced by STT series.

ference is that [44] handles the sequential input with LSTM blocks.

Self-attention among Pixels Sinusoidal positional encoding is adopted here for texts on all of the models. As for visual feature maps, we form a 1024-dimensional vector to represent its vertical position, and another 1024-dimensional vector for its horizontal position, then concatenate these two vectors as final 2048-dimensional position feature vector.

Pre-training and Beam Search Firstly, rather than training a new model from scratch, we also adopt a Resnet-101 pre-trained on Imagenet to be the image encoder, with the last two layers being replaced by down-sampling convolution, and it will be fine-tuned with COCO dataset. Secondly, to improve efficiency and preserve the results, we take the pre-trained GLOVE [31] for word embedding. To be noticed, it’s not a common NLP practice because the pre-training is not carried out on the modules for alignment. Besides, Beam Search is adopted to alleviate computation burden. It executes graph search on a limited sub-optimal set, which saves a lot of time for all the models.

4.2.2 Metrics

The results are reported under standard evaluation protocol, where captioning metrics including full set of BLEU [23], along with METEOR [11], CIDEr [38], ROUGE [26]. Most of them are based on n -gram to evaluate the quality of the generated sentences with ground truths, and they complement with each other to yield fairer results.

4.2.3 Quantitative Analysis of Image Captioning

The performance quantified by the seven metrics is summarized in Table 6, from which we can see that both of LSTM-based and transformer-based image captioning framework perform worse than STT series for all seven metrics. It is interesting that LSTM-based model appears to be inferior to transformer-based models, given that transformer frees the model from sequential input dependence. Furthermore, all of modules from STT series tend to improve the results than traditional methods. Besides, MS (Tensor Mixture Synthesizer) seems to achieve most of the best results among the model zoo. Moreover, in comparison with baseline caption models with LSTM and Transformer, both SR (Tensor Random Synthesizer) and FSR (Tensor Factorized Random Synthesizer) yield better results with less time for testing, and fewer parameters. The alignments in transformer are conducted on one side of the feature map while dense synthesizer enables a competitive attention for three sides of the feature tensor, which might result in the overall performance superiority of STT against the baselines.

5 Conclusion

In this paper, we present a self-attention plug-in module with its variants, named the series of **STT**. It employs the tensor transformation for self-alignment to replace the traditional dot-product multiplication in the self-attention module. Through this novel approach, the shortage of exhaustive and redundant computation caused by dot-production is dramatically mitigated. In our image caption experiments,

the **STT** series achieve most of the best results with less time in testing, and use fewer parameters. Moreover, because the synthesizing mechanism notably reduces the input feature’s reliance, the underlying structure is preserved. The **STT** series strongly facilitate the robustness of the baseline model. In the image classification experiments, the **STT** series represent the competitive robustness encountering multiple external perturbations. It demonstrates the **STT** series have the potential to improve the robustness, lower the overfitting, and the flexibility to be extended to more deep learning architectures.

References

- [1] Jimmy Ba, Volodymyr Mnih, and Koray Kavukcuoglu. Multiple object recognition with visual attention. In *ICLR*, 2015. 1
- [2] Irwan Bello, Barret Zoph, Ashish Vaswani, Jonathon Shlens, and Quoc V Le. Attention augmented convolutional networks. In *ICCV*, pages 3286–3295, 2019. 2, 3
- [3] Nicolas Carion, Francisco Massa, Gabriel Synnaeve, Nicolas Usunier, Alexander Kirillov, and Sergey Zagoruyko. End-to-end object detection with transformers. In *ECCV*, volume 12346, pages 213–229, 2020. 2
- [4] Long Chen, Hanwang Zhang, Jun Xiao, Liqiang Nie, Jian Shao, Wei Liu, and Tat-Seng Chua. Sca-cnn: Spatial and channel-wise attention in convolutional networks for image captioning. In *CVPR*, pages 5659–5667, 2017. 2
- [5] Mark Chen, Alec Radford, Rewon Child, Jeffrey Wu, Heewoo Jun, David Luan, and Ilya Sutskever. Generative pretraining from pixels. In *ICML*, pages 1691–1703, 2020. 2
- [6] Xinlei Chen, Hao Fang, Tsung-Yi Lin, Ramakrishna Vedantam, Saurabh Gupta, Piotr Dollár, and C Lawrence Zitnick. Microsoft coco captions: Data collection and evaluation server. *arXiv preprint arXiv:1504.00325*, 2015. 9
- [7] Yunpeng Chen, Yannis Kalantidis, Jianshu Li, Shuicheng Yan, and Jiashi Feng. A²-nets: Double attention networks. In *NIPS*, pages 350–359, 2018. 3
- [8] Krzysztof Marcin Choromanski, Valerii Likhoshersov, David Dohan, Xingyou Song, Andreea Gane, Tamás Szepesvári, Peter Hawkins, Jared Quincy Davis, Afroz Mohiuddin, Lukasz Kaiser, David Benjamin Belanger, Lucy J. Colwell, and Adrian Weller. Rethinking attention with performers. In *ICLR*, 2021. 1
- [9] Jean-Baptiste Cordonnier, Andreas Loukas, and Martin Jaggi. On the relationship between self-attention and convolutional layers. In *ICLR*, 2020. 2, 3
- [10] Lieven De Lathauwer, Bart De Moor, and Joos Vandewalle. A multilinear singular value decomposition. *SIAM journal on Matrix Analysis and Applications*, 21(4):1253–1278, 2000. 3
- [11] Michael Denkowski and Alon Lavie. Meteor universal: Language specific translation evaluation for any target language. In *Proceedings of the ninth workshop on statistical machine translation*, pages 376–380, 2014. 10
- [12] Yihe Dong, Jean-Baptiste Cordonnier, and Andreas Loukas. Attention is not all you need: pure attention loses rank doubly exponentially with depth. In *ICML*, volume 139, pages 2793–2803, 2021. 1
- [13] Alexey Dosovitskiy, Lucas Beyer, Alexander Kolesnikov, Dirk Weissenborn, Xiaohua Zhai, Thomas Unterthiner, Mostafa Dehghani, Matthias Minderer, Georg Heigold, Sylvain Gelly, Jakob Uszkoreit, and Neil Houlsby. An image is worth 16x16 words: Transformers for image recognition at scale. In *ICLR*, 2021. 2, 3
- [14] Shahriar Rahman Fahim, Yeahia Sarker, Subrata K. Sarker, Md. Rafiqul Islam Sheikh, and Sajal K. Das. Self attention convolutional neural network with time series imaging based feature extraction for transmission line fault detection and classification. *Electric Power Systems Research*, 187:106437, 2020. 1
- [15] Jun Fu, Jing Liu, Haijie Tian, Yong Li, Yongjun Bao, Zhiwei Fang, and Hanqing Lu. Dual attention network for scene segmentation. In *CVPR*, pages 3146–3154, 2019. 2
- [16] Jonathan Ho, Nal Kalchbrenner, Dirk Weissenborn, and Tim Salimans. Axial attention in multidimensional transformers. *arXiv preprint arXiv:1912.12180*, 2019. 2
- [17] Han Hu, Jiayuan Gu, Zheng Zhang, Jifeng Dai, and Yichen Wei. Relation networks for object detection. In *CVPR*, pages 3588–3597, 2018. 2
- [18] Jie Hu, Li Shen, Samuel Albanie, Gang Sun, and Andrea Vedaldi. Gather-excite: Exploiting feature context in convolutional neural networks. In *NIPS*, pages 9423–9433, 2018. 2

- [19] Jie Hu, Li Shen, and Gang Sun. Squeeze-and-excitation networks. In *CVPR*, pages 7132–7141, 2018. **1, 2**
- [20] Lun Huang, Wenmin Wang, Jie Chen, and Xiaoyong Wei. Attention on attention for image captioning. In *ICCV*, pages 4633–4642, 2019. **1**
- [21] Lang Huang, Yuhui Yuan, Jianyuan Guo, Chao Zhang, Xilin Chen, and Jingdong Wang. Interlaced sparse self-attention for semantic segmentation. *arXiv preprint arXiv:1907.12273*, 2019. **2**
- [22] Zilong Huang, Xinggang Wang, Lichao Huang, Chang Huang, Yunchao Wei, and Wenyu Liu. Cnet: Criss-cross attention for semantic segmentation. In *ICCV*, pages 603–612, 2019. **3**
- [23] Andrej Karpathy and Li Fei-Fei. Deep visual-semantic alignments for generating image descriptions. In *CVPR*, pages 3128–3137, 2015. **10**
- [24] Nikita Kitaev, Lukasz Kaiser, and Anselm Levskaya. Reformer: The efficient transformer. In *ICLR*, 2020. **1, 3**
- [25] Alex Krizhevsky, Geoffrey Hinton, et al. Learning multiple layers of features from tiny images. 2009. **7**
- [26] Chin-Yew Lin. Rouge: A package for automatic evaluation of summaries. In *Text summarization branches out*, pages 74–81, 2004. **10**
- [27] Chenxi Liu, Junhua Mao, Fei Sha, and Alan L. Yuille. Attention correctness in neural image captioning. In *AAAI*, pages 4176–4182, 2017. **2**
- [28] Volodymyr Mnih, Nicolas Heess, Alex Graves, et al. Recurrent models of visual attention. In *NIPS*, pages 2204–2212, 2014. **1**
- [29] Niki Parmar, Prajit Ramachandran, Ashish Vaswani, Irwan Bello, Anselm Levskaya, and Jon Shlens. Stand-alone self-attention in vision models. In *NIPS*, pages 68–80, 2019. **2, 3**
- [30] Niki Parmar, Ashish Vaswani, Jakob Uszkoreit, Lukasz Kaiser, Noam Shazeer, Alexander Ku, and Dustin Tran. Image transformer. In *ICML*, pages 4055–4064, 2018. **2**
- [31] Jeffrey Pennington, Richard Socher, and Christopher D Manning. Glove: Global vectors for word representation. In *EMNLP*, pages 1532–1543, 2014. **10**
- [32] Jack W. Rae, Anna Potapenko, Siddhant M. Jayakumar, Chloe Hillier, and Timothy P. Lillicrap. Compressive transformers for long-range sequence modelling. In *ICLR*, 2020. **1**
- [33] Aurko Roy, Mohammad Saffar, Ashish Vaswani, and David Grangier. Efficient content-based sparse attention with routing transformers. *Trans. Assoc. Comput. Linguistics*, 9:53–68, 2021. **1**
- [34] Matthias Seibert, Julian Wörmann, Rémi Gribonval, and Martin Kleinsteuber. Learning co-sparse analysis operators with separable structures. *IEEE Transactions on Signal Processing*, 64(1):120–130, 2015. **3, 4**
- [35] Yi Tay, Dara Bahri, Donald Metzler, Da-Cheng Juan, Zhe Zhao, and Che Zheng. Synthesizer: Rethinking self-attention in transformer models, 2020. **1, 2, 7, 8**
- [36] Charles F Van Loan. The ubiquitous kronecker product. *Journal of computational and applied mathematics*, 123(1-2):85–100, 2000. **3, 6**
- [37] Ashish Vaswani, Noam Shazeer, Niki Parmar, Jakob Uszkoreit, Llion Jones, Aidan N Gomez, Lukasz Kaiser, and Illia Polosukhin. Attention is all you need. In *NIPS*, pages 5998–6008, 2017. **7, 8**
- [38] Ramakrishna Vedantam, C Lawrence Zitnick, and Devi Parikh. Cider: Consensus-based image description evaluation. In *CVPR*, pages 4566–4575, 2015. **10**
- [39] Fei Wang, Mengqing Jiang, Chen Qian, Shuo Yang, Cheng Li, Honggang Zhang, Xiaogang Wang, and Xiaoou Tang. Residual attention network for image classification. In *CVPR*, 2017. **1, 2**
- [40] Huiyu Wang, Yukun Zhu, Bradley Green, Hartwig Adam, Alan Yuille, and Liang-Chieh Chen. Axial-deeplab: Stand-alone axial-attention for panoptic segmentation, 2020. **2**
- [41] Sinong Wang, Belinda Z. Li, Madian Khabsa, Han Fang, and Hao Ma. Linformer: Self-attention with linear complexity, 2020. **1, 3, 7, 8**
- [42] Sanghyun Woo, Jongchan Park, Joon-Young Lee, and In So Kweon. Cbam: Convolutional block attention module. In *ECCV*, 2018. **1, 2**
- [43] Qingyang Wu, Zhenzhong Lan, Jing Gu, and Zhou Yu. Memformer: The memory-augmented transformer, 2020. **1**
- [44] Kelvin Xu, Jimmy Ba, Ryan Kiros, Kyunghyun Cho, Aaron Courville, Ruslan Salakhudinov, Rich Zemel, and Yoshua Bengio. Show, attend and tell: Neural image caption generation with visual attention. In *ICML*, pages 2048–2057, 2015. **9, 10**
- [45] Manzil Zaheer, Guru Guruganesh, Avinava Dubey, Joshua Ainslie, Chris Alberti, Santiago Ontanon, Philip Pham, Anirudh Ravula, Qifan Wang, Li Yang, and Amr Ahmed. Big bird: Transformers for longer sequences. In *NIPS*, 2020. **1**

- [46] Hengshuang Zhao, Jiaya Jia, and Vladlen Koltun. Exploring self-attention for image recognition. In *CVPR*, pages 10076–10085, 2020. [2](#), [3](#)
- [47] Xizhou Zhu, Weijie Su, Lewei Lu, Bin Li, Xiaogang Wang, and Jifeng Dai. Deformable DETR: deformable transformers for end-to-end object detection. In *ICLR*, 2021. [1](#), [2](#)